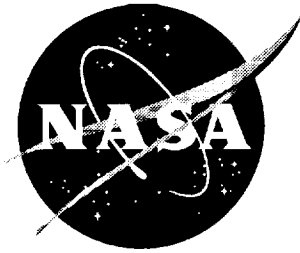


NASA/CR-1998-207641



Start Up of a Nb-1%Zr Potassium Heat Pipe From the Frozen State

David E. Glass

Analytical Services and Materials, Inc., Hampton, VA

Michael A. Merrigan, and J. Tom Sena

Los Alamos National Laboratory, Los Alamos, NM

National Aeronautics and
Space Administration

Langley Research Center
Hampton, Virginia 23681-2199

Prepared for Langley Research Center
under Contract NAS1-19317

March 1998

ical Information Service (NTIS)
Road
22161-2171

Available from the following:

NASA Center for AeroSpace Information (CASI)
800 Elkridge Landing Road
Linthicum Heights, MD 21090-2934
(301) 621-0390

National Techn
5285 Port Roya
Springfield, V
(703) 487-4650

Start Up of a Nb-1%Zr Potassium Heat Pipe

From the Frozen State

David E. Glass
Analytical Services & Materials, Inc., Hampton, VA

Michael A. Merrigan and J. Tom Sena
Los Alamos National Laboratory, Los Alamos, NM

Abstract

The start up of a liquid-metal heat pipe from the frozen state was evaluated experimentally with a Nb-1%Zr heat pipe with potassium as the working fluid. The heat pipe was fabricated and tested at Los Alamos National Laboratory. RF induction heating was used to heat 13 cm of the 1-m-long heat pipe. The heat pipe and test conditions are well characterized so that the test data may be used for comparison with numerical analyses. An attempt was made during steady state tests to calibrate the heat input so that the heat input would be known during the transient cases. The heat pipe was heated to 675°C with a throughput of 600 W and an input heat flux of 6 W/cm². Steady state tests, start up from the frozen state, and transient variations from steady state were conducted.

Nomenclature

English

L	length
•	
m	mass flow rate
PS	power setting
r	radius
q	heat flux
q''	heat flux per unit area
T	temperature
v	voltage
V	volume
x	axial location on heat pipe

Greek

ε	porosity
ρ	resistivity

Subscripts

e	evaporator
end cap	end cap on heat pipe
f	final
plug	plug in heat pipe

Introduction

Since the working fluid in a liquid-metal heat pipe is frozen at room temperature, the start up is an important consideration in any application of liquid-metal heat pipes. However, experimental data for the transient start up of liquid-metal heat pipes is limited. Merrigan, et. al, [1-2] studied the start-up and shut-down performance of a molybdenum-lithium heat pipe at temperatures to 1500K. It was indicated that liquid depletion in the evaporator region could occur during shut-down and prevent the restart of the heat pipe. The radial power density in the condenser and the relative radial power density in the evaporator and condenser are important considerations in the restart of a heat pipe. Wojcik and Clark [3] designed, analyzed, and tested several niobium-lithium heat pipes and tested a niobium alloy (C-103) "D-shaped" heat pipe in an oxidizing atmosphere. The heat pipe was coated with a silicide coating and was heated with a gas welding torch. Camarda [4] tested a wing-leading-edge segment cooled with Hastelloy X-sodium heat pipes. The heat pipes operated properly and no start up or other limiting conditions developed during testing. Large temperature gradients were observed during the start up, which could result in large thermal stresses. Several "D-shaped" Mo-Re heat pipes with lithium working fluid have been fabricated and tested by Glass, et al. [5]. They present limited steady state and start-up data for a 30-in-long heat pipe.

The present paper presents experimental data obtained at Los Alamos National Laboratory (LANL) for the start up of a Nb-1%Zr heat pipe with potassium (K) as the working fluid. The heat pipe was fabricated by LANL for heat flux limit tests and had been tested several times prior to the current tests. Radial heat fluxes of 147 W/cm^2 were obtained during the prior tests with this heat pipe at a vapor temperature of 925K [6]. The heat flux value was approximately five times greater than the previously accepted experimentally obtained design limit for potassium heat pipes. The heat pipe had an annular geometry and was initially charged with lithium. Pre-testing with lithium was performed to improve the wetting characteristics of the heat-pipe inner wall, and thus reduce to a minimum the largest active nucleation site radius. An analytical model for predicting boiling limits was also determined from previous testing on the heat pipe at LANL [7]. A nucleation site radius of $3 \mu\text{m}$ appeared to correlate very well with the experimental data.

In the current study, several different types of start-up transients were evaluated. These included start up from the frozen state as well as perturbations of the heat flux while at steady state conditions. Steady state tests were also conducted to assist in the estimation of the applied heat flux during transient conditions.

Heat-Pipe Description

The heat pipe used for this experiment was fabricated from a 1-m-long segment of Nb-1%Zr tubing drawn down to a 0.775-cm-outside radius and a 0.127-cm wall thickness. The wick was fabricated from a single piece of 100-mesh plain, square-weave Nb-1%Zr screen. Three layers of the screen were wrapped around a 0.559-cm radius mandrel as shown in Figure 1. The mandrel and screen were then inserted in a tube with a 0.7938-cm-outside radius and a 0.089-cm wall thickness. The outer tube was then drawn down to a 0.6895-cm-outer radius, thus compressing the screen wick. In the compressed state, the wick was 0.038-cm thick with an experimentally determined pore diameter of $1.3 \times 10^{-5} \text{ m}$. The screen was further treated by vacuum firing to remove volatile contaminants.

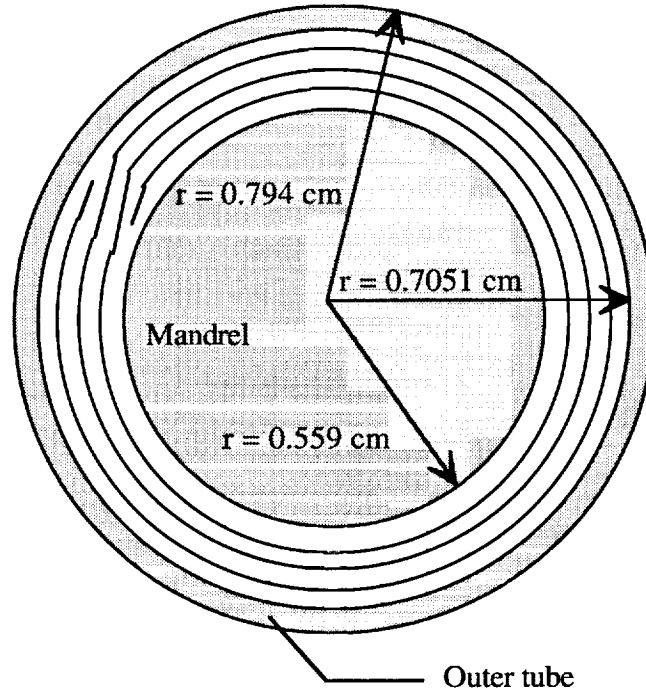


Figure 1: Schematic diagram of mandrel, screen wick, and outer tube used to compress the screen wick.

The compressed screen, with an inner radius of 0.559 cm and an outer radius of 0.597 cm, was then inserted into the heat-pipe container, with an inner radius of 0.648 cm, as shown in Figure 2. This resulted in forming a 0.051-cm annulus between the container and the tubular wick. The 0.051-cm annulus served as a path for fluid return from the condenser to the evaporator during operation. A Nb-1%Zr plug was used to close the screen wick at the evaporator end. This plug closure was necessary to ensure that the longitudinal pumping capability was established by the effective pore size of the screen wick rather than by the annular gap thickness. The plug added a significant thermal mass to the heat pipe and thus effected the start-up characteristics of the heat pipe. The length of the plug was 1.27 cm. The diameter of the plug was equal to the inside diameter of the screen wick, and was thus 0.559 cm. Thus, the volume of the plug was

$$V_{\text{plug}} = \pi r^2 L_{\text{plug}} = \pi (0.559 \text{ cm})^2 \times 1.27 \text{ cm} = 1.25 \text{ cm}^3$$

In addition to the plug in the screen, there is an end cap in the heat pipe. The length of the end cap is estimated to be 0.64 cm. The volume of the end cap was thus

$$V_{\text{end cap}} = \pi r^2 L_{\text{end cap}} = \pi (0.648 \text{ cm})^2 (0.64 \text{ cm}) = 0.84 \text{ cm}^3$$

The total additional volume of Nb-1%Zr at the evaporator end of the heat pipe was thus

$$V = V_{\text{plug}} + V_{\text{end cap}} = 1.25 \text{ cm}^3 + 0.84 \text{ cm}^3 = 2.09 \text{ cm}^3$$

The wire diameter of the screen was measured to be 0.0076 cm. The porosity of the uncompressed wick can be calculated by dividing the void volume by the total volume in a unit cell of 1-cm² area and one layer of screen thick. With a measured screen thickness of

0.0203 cm, a wire diameter of 0.0076 cm, and 39.37 wires/cm (100 mesh screen) the screen volume was

$$[1 \text{ cm} \times 39.37 \text{ wires} \times 2] \times (0.0076 \text{ cm})^2 \times \pi / 4 = 0.0036 \text{ cm}^3$$

The total volume in a unit cell was

$$1 \text{ cm} \times 1 \text{ cm} \times 0.0203 \text{ cm} = 0.0203 \text{ cm}^3$$

The porosity of the uncompressed screen was thus

$$\epsilon = 1 - \frac{0.0036 \text{ cm}^3}{0.0203 \text{ cm}^3} = 0.823$$

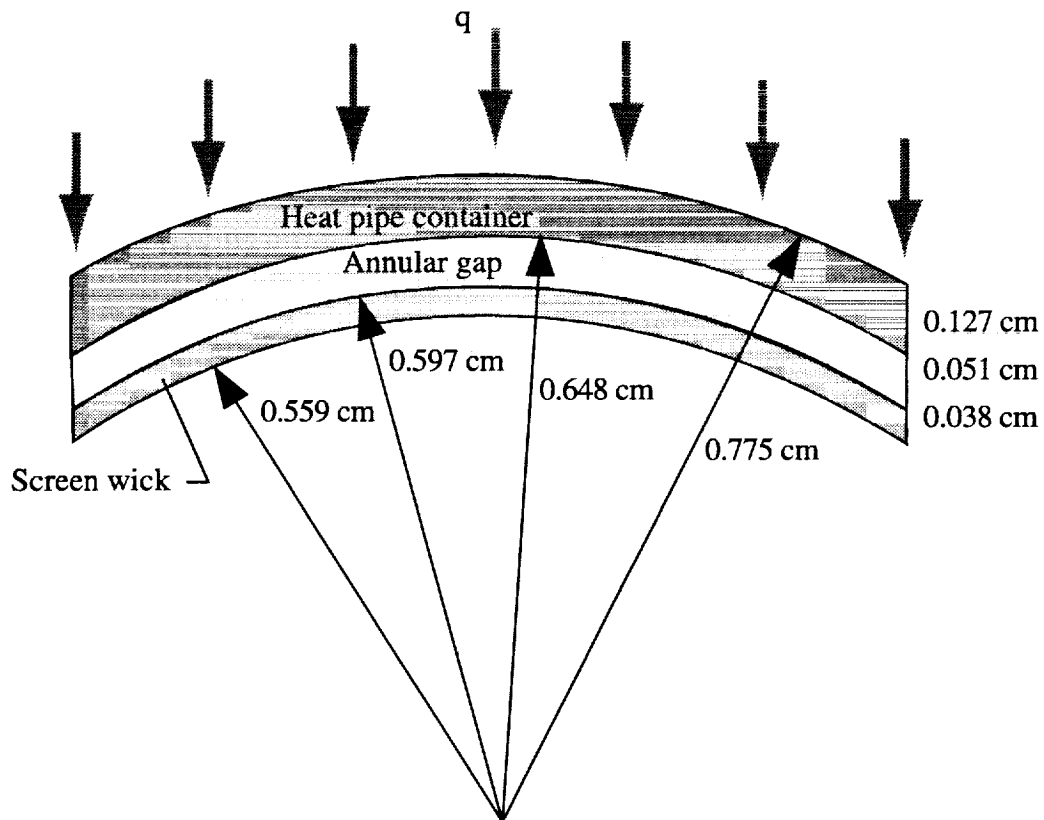


Figure 2: Schematic diagram of actual heat pipe showing annular gap and screen wick.

Test Setup

A vacuum chamber was used for the heat-pipe testing. A 10-cm long rf induction coil was used for heating the evaporator. The heat pipe was instrumented with sixteen thermocouples spot welded to the surface of the heat pipe for temperature monitoring. The condenser portion of the heat pipe was covered by a single pass water calorimeter. The heat-pipe throughput was determined by measuring the change in water temperature and flow through the calorimeter. A schematic of the test setup, showing the vacuum chamber, heat pipe, calorimeter, and induction heating coils is shown in Figure 3.

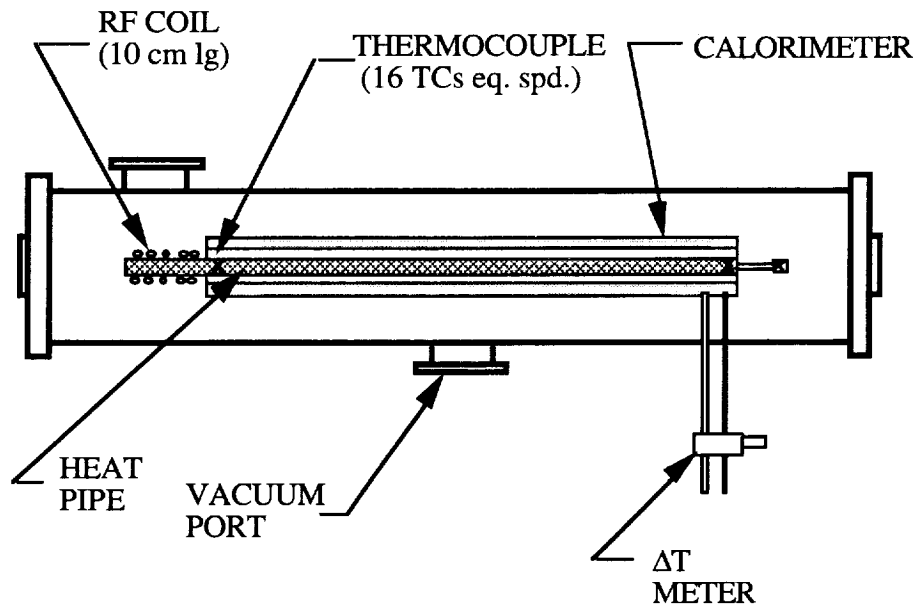


Figure 3: Schematic drawing of the vacuum chamber, heat pipe, and calorimeter used for the heat-pipe tests.

The heat pipe was 1-m long and was heated over a 10-cm length 3 cm from the end of the heat pipe, as shown in Figure 4. The induction coils were fabricated out of 0.635-cm-diameter copper tubing and had an inner diameter of 2.8 cm. Fourteen coils were used over the 10-cm-evaporator length. A 100 kW generator with a 300 kHz rating was used for the power supply.

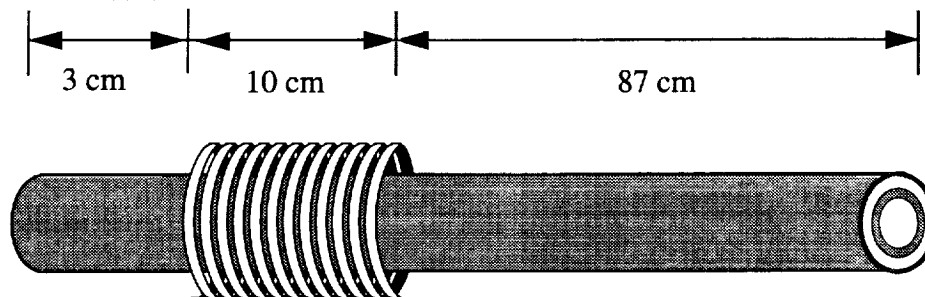


Figure 4: Schematic drawing of the heat pipe and the induction heating coils.

Sixteen thermocouples were placed on the heat pipe and were equally spaced in the 87-cm long condenser region. The first thermocouple was located at the edge of the induction coils, $x = 13$ cm. The thermocouple spacing was 5.8 cm, with the final thermocouple (TC #16) located at the end of the 1-m-long heat pipe.

Discussion and Results

Before the heat pipe was performance tested, it was “wet-in” in a horizontal position. The “wet-in” procedure consisted of heating the entire heat pipe at 550-600°C for 50 hours and helped ensure the working fluid was uniformly distributed within the heat pipe.

A slow start-up test was conducted to verify heat-pipe operation. Heat was applied to the heat pipe at a slow rate until the heat pipe was isothermal at 600°C. The heat pipe was operated with calorimetry to determine the heat-pipe throughput. There was no indication of gas contamination or abnormal operation of the heat pipe after stabilization at 600°C.

This test was followed with a steady-state test designed to determine heat input flux at corresponding power settings. This was accomplished by increasing the input power to a known power setting and allowing the heat pipe to reach steady state and recording the power throughput. The process was repeated and the final test was conducted with the heat-pipe temperature of 675°C and a throughput of 600 W. The temperature distributions for each of the tests are shown in Figure 5 for power settings (PS) from 2.56 to 0. At a power setting of 0, heat was applied to the heat pipe. However, as can be seen in the figure, the heat pipe was not isothermal and was thus not operating as a heat pipe.

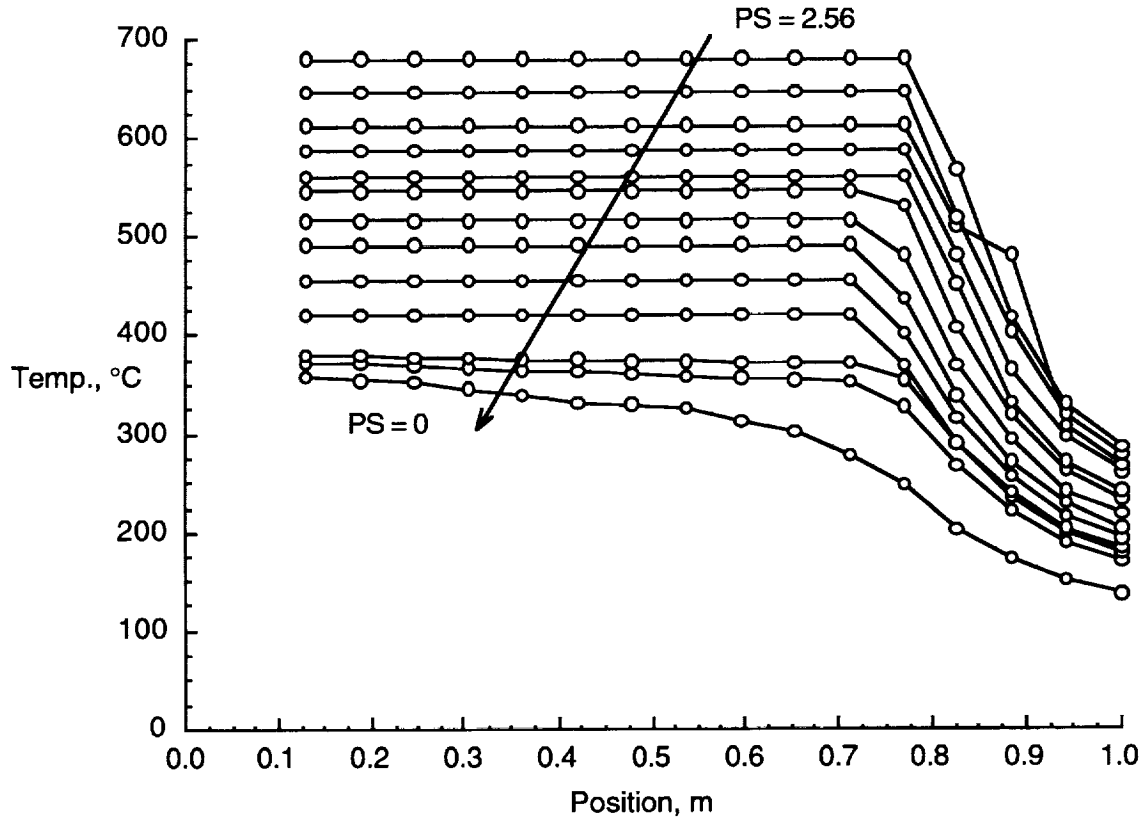


Figure 5: Steady state temperature distributions corresponding to tests listed in Table 1.

The throughput and steady state temperatures for each of the tests shown in Figure 5 are listed in Table 1. Since at a PS = 0 the heat pipe was not isothermal, no temperature is given in the table. For all except two of the tests, the water flow rate was approximately 50 g/sec. At a power setting of PS = 2.2, tests were run with flow rates of 50.6 g/sec and 96 g/sec, with both resulting in the same steady state temperatures, but slightly different throughputs. Thus, only one plot for the steady state temperature at PS = 2.2 is shown in Figure 5. The throughput of the heat pipe was calculated from

$$q = \dot{m} v 10.41$$

where the throughput q is in Watts, \dot{m} is the coolant mass flow rate in grams/sec, and v is the voltage from the calorimeter in mV.

During steady state tests, the heat input to the heat pipe can be determined from an energy balance using the throughput. However, during transients, not all the heat into the heat pipe leaves the heat pipe. Thus an attempt was made to calibrate the power settings so that the heat flux could be estimated during the transients based on the power settings. The

steady state throughput was curve fit with a fourth order polynomial to estimate the input to the heat pipe at various power settings. The curve fit is given by

$$q = -5058.2 + 1.0758 \times 10^4 \text{ PS} - 8560.2 \text{ PS}^2 + 3046.3 \text{ PS}^3 - 393.28 \text{ PS}^4 \quad (1)$$

The heat input rate to the heat pipe was then determined by dividing the total throughput by the heat-pipe surface area under the evaporator coils. With an evaporator length $L_e = 10 \text{ cm}$ and an outer radius of $r = 0.775 \text{ cm}$, the heat flux was determined from

$$q'' = \frac{q}{2\pi r L_e} \quad (2)$$

Table 1: Throughput and Steady State Temperatures of Heat Pipe as Shown in Figure 5

Power Setting	Volts, mV	\dot{m} , g/sec	Throughput, W	Temp, °C
0.0	0.176	50.5	92.52	-
1.5	0.213	50.0	110.87	365
1.55	0.233	50.0	121.28	380
1.65	0.294	50	153.03	420
1.75	0.368	50	191.54	455
1.85	0.452	50	235.27	490
1.95	0.516	50	268.58	520
2.05	0.611	50	318.03	550
2.1	0.652	50	339.37	565
2.2	0.758	50.6	399.27	590
2.2	0.41	96	409.74	590
2.3	0.47	96	469.70	615
2.46	1.027	50.6	540.97	655
2.56	1.142	50.6	601.54	675

As mentioned previously, the heat pipe was heated with induction heating. Though induction heating is an excellent method to apply heat to heat pipes, it does enter some uncertainty into the heat flux estimates during transient conditions. During the transient tests, the power setting (potentiometer) was changed in steps. The control system, however, controls the high voltage available to the oscillator tube rather than the output power. [8] With a constant value of high voltage, there is a complex interaction between the load resistance (proportional to pipe resistivity), the tuned tank oscillating current, and the pipe power deposition. When rf power is applied with the heat pipe at ambient temperature, the power input to the heat pipe is the appropriate value for the Nb-1%Zr ambient-temperature resistivity. As the temperature and resistivity of the heat pipe rise, the input power correspondingly rises. Thus, when power is supplied to the system with the potentiometer power setting at 1.6, the heat flux does not instantaneously jump to 2.89 W/cm^2 , but rather rises to that value as a function of the resistivity (and thus temperature) of the heat pipe. An estimate of how the heat flux rises as a function of heat-pipe temperature can be obtained [8]. The resistivity of niobium is a function of temperature and is given by

$$\rho = 13.3 + 0.0412 T \quad (3)$$

where ρ is the resistivity in $\mu\Omega\text{-cm}$ and T is the niobium temperature in °C. The equation used to calculate the heat-pipe transient power input, q'' , is

$$q'' = q''_f - [(\rho_f - \rho) \Delta q'' / \Delta \rho] \quad (4)$$

where q''_f is the final power input with the heat pipe at the final temperature. The gradient value $\Delta q'' / \Delta \rho$ can be obtained from the polynomial curve fit

$$\Delta q'' / \Delta \rho = -0.00754 - 0.0367 \text{ PS} + 0.03963 \text{ PS}^2 \quad (5)$$

where PS is the power setting on the potentiometer. The maximum error for the polynomial curve fit is 10%.

Following the steady-state tests, a series of transient tests were conducted. The data acquired from the steady state tests were used to estimate the heat flux corresponding to the power settings used during the transients test. Table 2 lists the power settings and corresponding throughput and heat flux over the range of the tests. The throughput values are estimated from Eq. (2) and do not attempt the transient correction in Eq. (4).

Table 2: Steady State Throughput and Heat Input to Heat Pipe Calculated From Equation

Power Setting	Throughput, (W)	Input (W/cm ²)
0.0	92.52	1.90
1.5	108.63	2.23
1.6	140.73	2.89
1.7	173.18	3.56
1.8	208.68	4.29
1.9	248.99	5.11
2.0	294.92	6.06
2.1	346.35	7.11

The transient tests were conducted by varying the amount and the rate of heat input during start up as well as perturbing the heat flux slightly at steady state. The steady state heat input estimated from Eq. (2) is given in Table 3 for each test as a function of time. An effort was made to keep the test times as short as reasonable (minutes instead of hours) to facility the use of the data to validate numerical models. Tests 1-4 all consisted of start up from the frozen state. In each case, the heat pipe was initially at room temperature, and at time equal 0, the heat flux was increased to the value given in the Table 3. Test 1 steps up to the maximum heat flux over several increments, while Test 2 consisted of maintaining the same heat flux throughout the entire test. Test 3 consisted of a large number of incremental increases in the heat flux occurring more rapidly than in Test 1. Test 4 consisted of a step up and then a step down in the applied heat flux. The final test was a transient test where the heat pipe was initially at a temperature of 565°C with an applied heat flux of 7.11 W/cm². The heat flux was then decreased and increased several times before finally being turned off.

The first transient test was a start up from the frozen state, periodically increasing the applied heat flux from 2.89 W/cm² to 6.06 W/cm². The times and heat fluxes are given in Table 3. After 1500 sec., the power was turned off and the heat pipe was allowed to cool to room temperature. If the power setting were turned back to 0 instead of cutting the power off, the heat flux would have been 1.9 W/cm² after 1500 sec. The start-up temperatures for Test 1 are shown in Figure 6 for the even numbered thermocouples (TC #2 through TC #16). The heat pipe reaches isothermal conditions through TC #10 ($x = 0.652$ m) prior to being shut down at 1500 sec. As was seen in Figure 5, even at steady state conditions, the heat pipe was isothermal only through TC #12 ($x = 0.768$ m).

Table 3: Estimated Applied Heat Flux as a Function of Time for Each Test

Time, sec.	Power Setting	Input (W/cm ²)
<u>Test #1</u>		
0	1.6	2.89
180	1.7	3.56
360	1.8	4.29
600	1.9	5.11
932	2.0	6.06
1500	off	0.0
<u>Test #2</u>		
0	1.6	2.89
1020	off	0.0
<u>Test #3</u>		
0	0.0	1.90
60	1.5	2.23
120	1.55	2.56
240	1.65	3.22
360	1.75	3.91
480	1.85	4.69
600	1.95	5.57
780	2.0	6.06
<u>Test #4</u>		
0	1.7	3.56
760	2.0	6.06
1358	1.7	3.56
1510	off	0.0
<u>Transient Test</u>		
<0	2.1	7.11
0	1.8	4.29
898	1.9	5.11
1539	1.7	3.56
2342	1.9	5.11
4267	1.8	4.29
4387	1.7	3.56
4507	1.6	2.89
4627	1.5	2.23
4747	off	0.0

Unlike Test 1, Test 2 maintained a constant heat flux of 2.89 W/cm² during the test. The transient temperatures are shown in Figure 7 for the even numbered thermocouples (TC #2 through TC #16). The heat pipe is nearly isothermal through TC #10, but some temperature variation can be seen in TC #2 through TC #10. Thermocouples #12 through 16 do not reach the isothermal operating temperature at any time during the tests.

Test 3 had the largest number of discrete increases in heat flux, as shown in Table 3. The temperature as a function of time for each of the 16 thermocouples is shown in Figure 8. At 1200 sec., the heat flux was increased from 6.06 W/cm² to 6.57 W/cm². Shortly after the increase, a hot spot appeared in the evaporator region. In an attempt to reduce the unknowns with the data, data is only presented in the figure prior to formation of the hot spot. Prior to the hot spot, TC #1 through TC #11 were all isothermal.

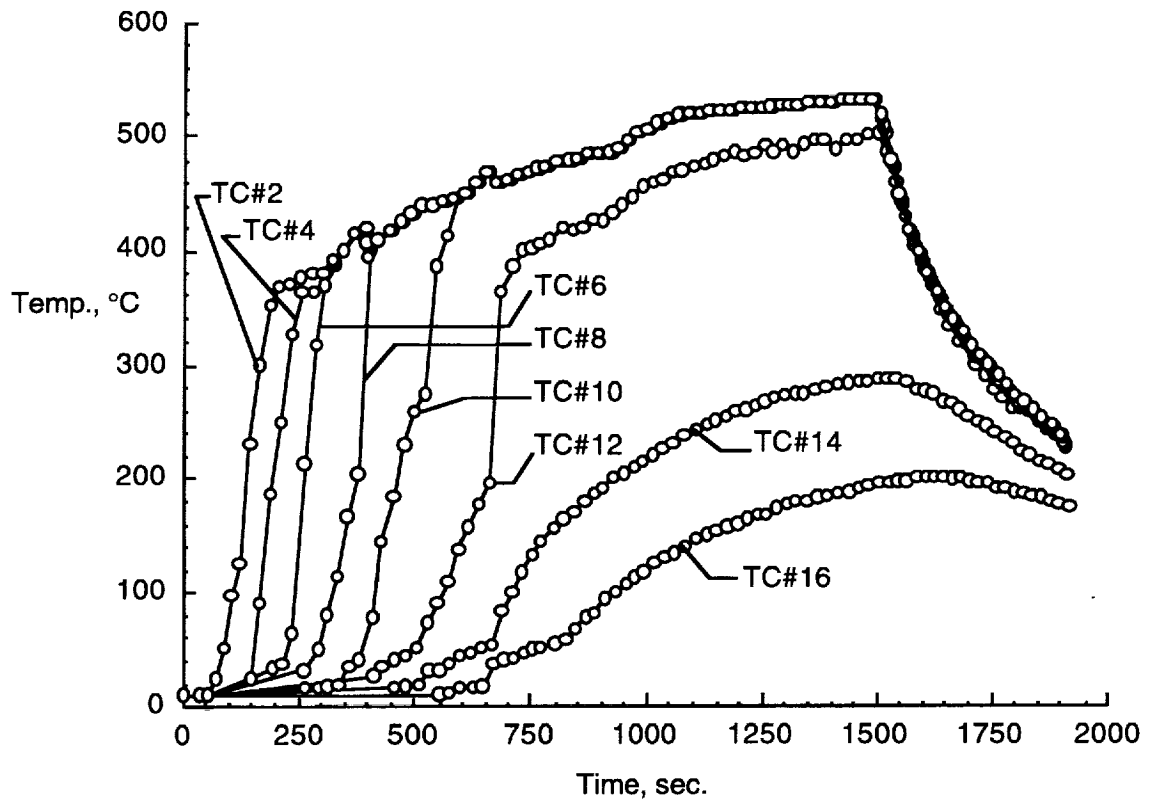


Figure 6: Temperature distributions for heat pipe start up from the frozen state (Test 1).

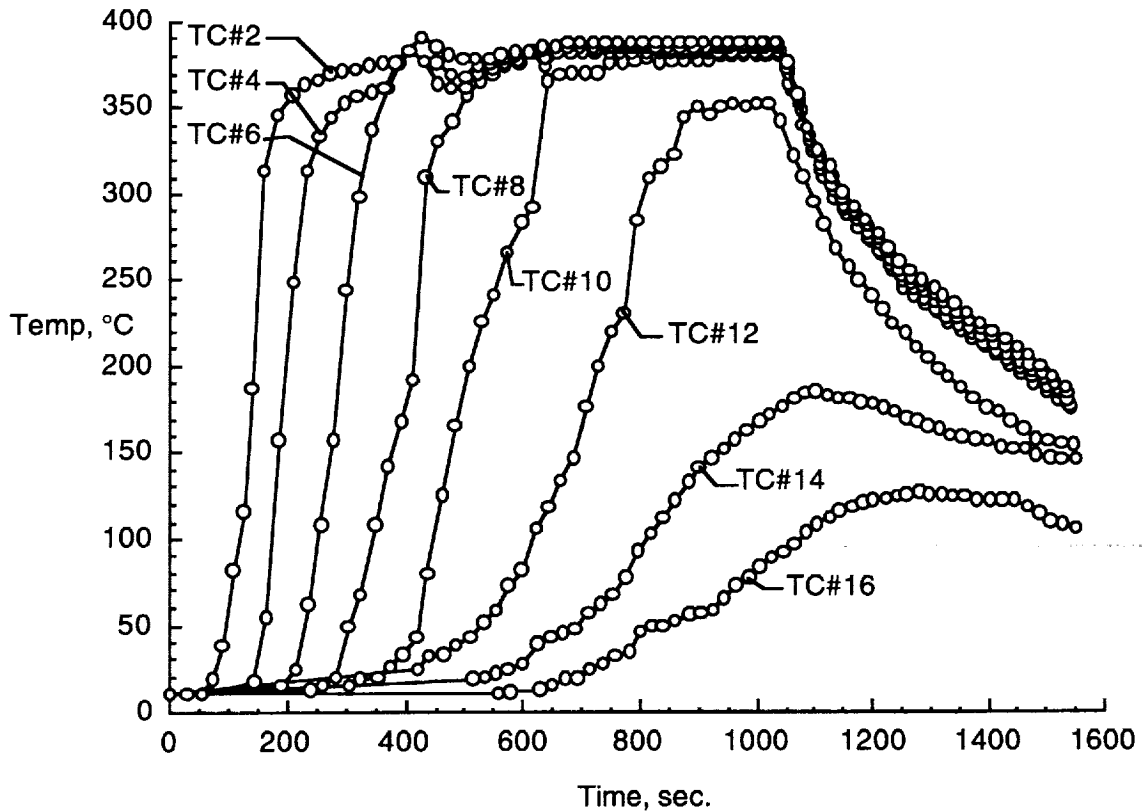


Figure 7: Temperature distributions for heat pipe start up from the frozen state (Test 2).

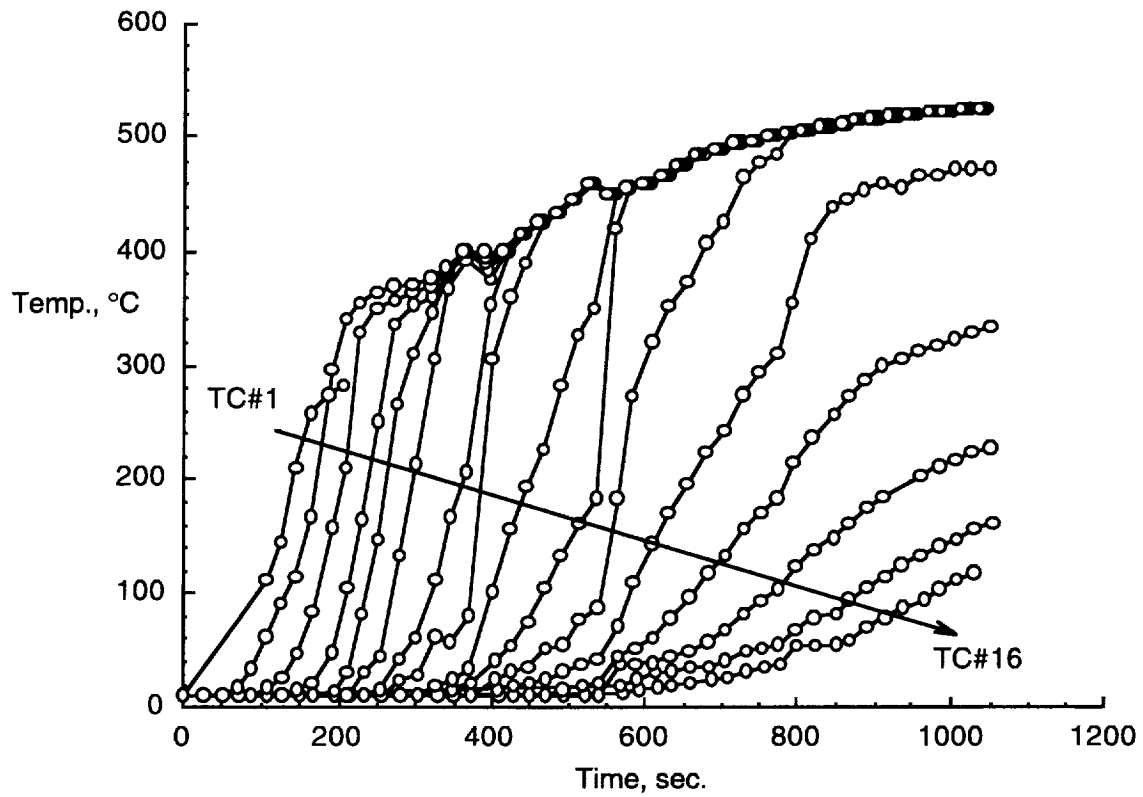


Figure 8: Temperature distributions for heat pipe start up from the frozen state (Test 3).

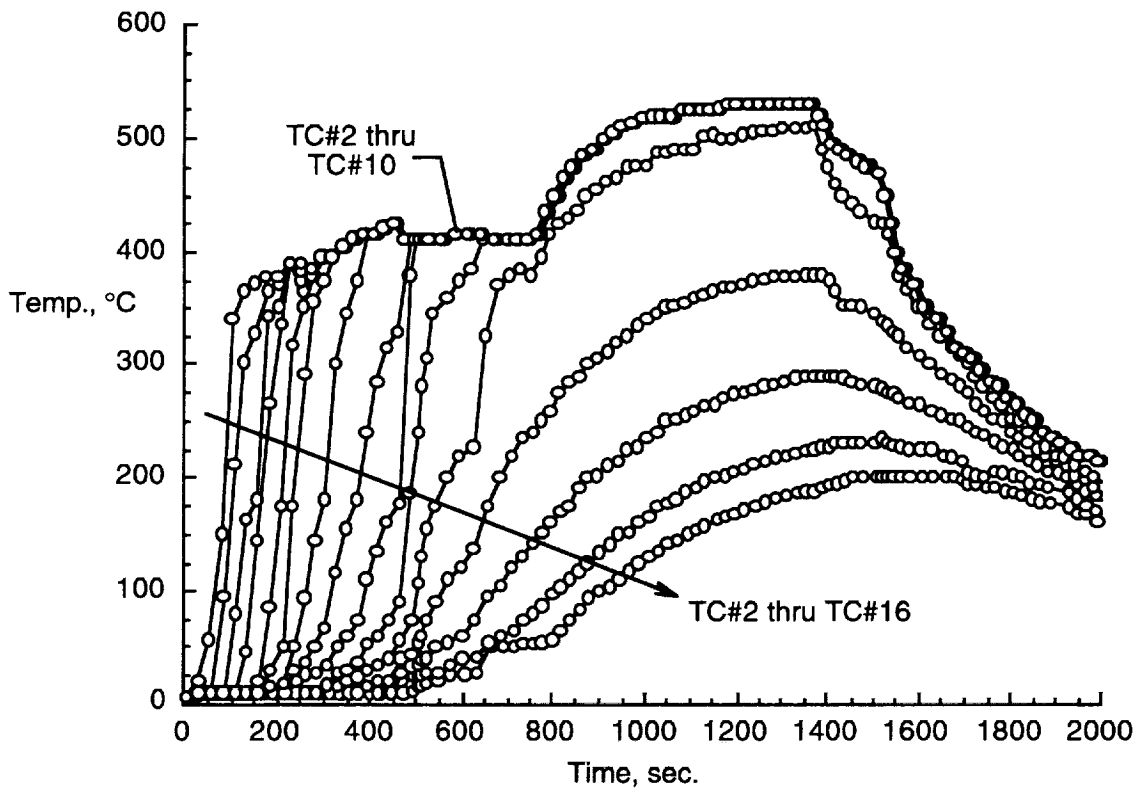


Figure 9: Temperature distributions for heat pipe start up from the frozen state (Test 4).

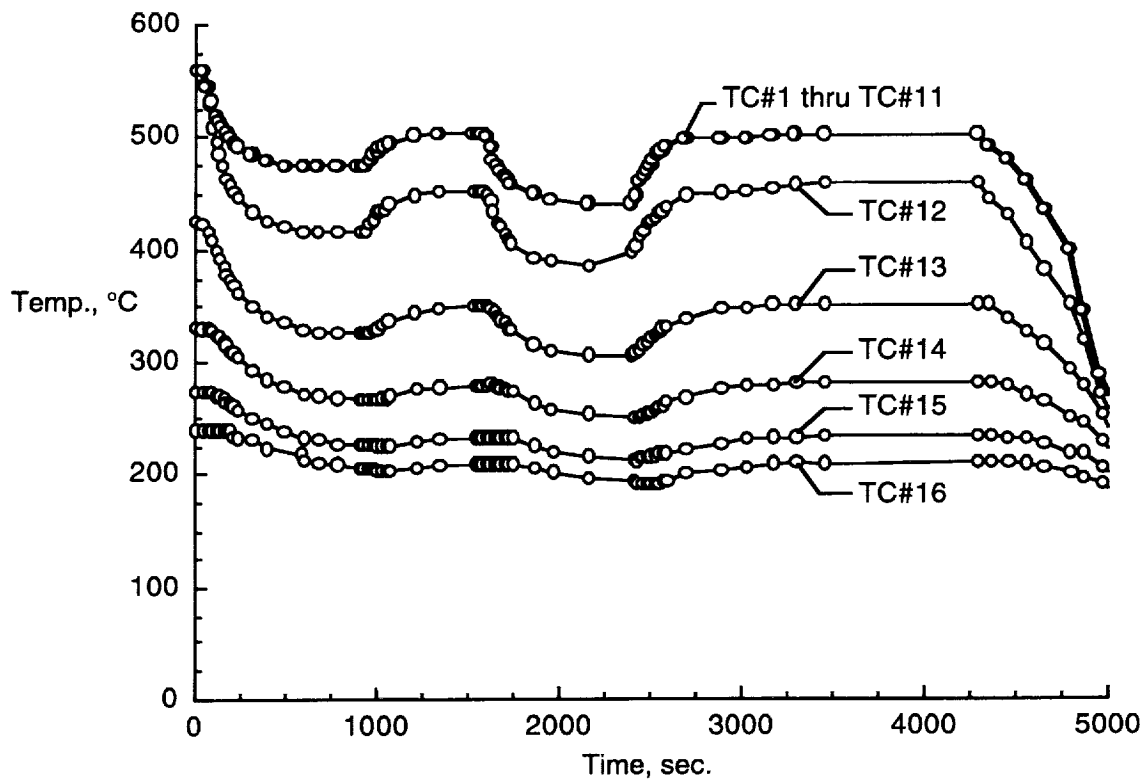


Figure 10: Temperature distributions for the heat pipe during transient testing.

In Test 4, the heat flux started out at 3.56 W/cm^2 , was increased to 6.06 W/cm^2 , and then was decreased back to 3.56 W/cm^2 before being turned off. Thermocouple #1 is not included with the transient data, shown in Figure 9, since it was not operating properly. Prior to increasing the heat flux to 6.06 W/cm^2 , the heat pipe was isothermal through TC #11. Even after the heat flux was increased to 6.06 W/cm^2 , TC #12 does not reach the isothermal temperature of the rest of the heat pipe.

One test is presented where the heat pipe was operating at steady state initially and the heat flux was then increased and decreased several times, as shown in Figure 10. The heat pipe was initially operating at a steady state temperature of 565°C (from Table 1) with a power setting of 2.1 ($q'' = 7.11 \text{ W/cm}^2$). Thermocouple #12 was nearly the same temperature as the isothermal portion of the heat pipe for $t < 0 \text{ sec.}$ Once the heat flux was dropped at $t = 0 \text{ sec.}$, the temperature at TC #12 rapidly dropped below that of the isothermal portion of the heat pipe. Since the heat flux was not increased back to the 7.11 W/cm^2 value, TC #12 never reached the heat-pipe operating temperature during this test. Thermocouple #1 through TC #11 remained isothermal throughout the test.

Concluding Remarks

A Nb-1%Zr heat pipe with potassium as the working fluid was tested under steady state, transient, and start-up conditions. The heat pipe was heated with induction heating up to a temperature of 675°C and a throughput of 600 W. The heat pipe and the test are well characterized so that the data may be used for comparison with analysis. The largest unknown in the test was the applied heat flux during the transient conditions.

Acknowledgment

The first author would like to thank NASA Langley Research Center for funding the heat-pipe testing under contract No. NAS1-19317 and Los Alamos National Laboratory for testing the heat pipe. The help of E. A. Brown of LANL on the variation of the applied heat flux with temperature is also appreciated.

References

1. Merrigan, M. A.; Keddy, E. S.; and Sena, J. T.: Transient Heat Pipe Investigations for Space Power Systems. Submitted to SP-100 Program Integration Meeting, Denver, CO, September 19, 1985. LA-UR-85-3341.
2. Merrigan, M. A.; Keddy, E. S.; and Sena, J. T.: Transient Performance Investigation of a Space Power System Heat Pipe. Presented at the AIAA/ASME 4th Joint Thermophysics and Heat Transfer Conference, Boston, MA, June 2-4, 1986. AIAA Paper No. 86-1273.
3. Wojcik, C; and Clark, L.: Design, Analysis, and Testing of Refractory Metal Heat Pipes Using Lithium as the Working Fluid. Presented at the AIAA 26th Thermophysics Conference, Honolulu, Hawaii, June 24-26, 1991. AIAA Paper No. 91-1400.
4. Camarda, Charles J.: Analysis and Radiant Heating Tests of a Heat-Pipe-Cooled Leading Edge. NASA TN D-8468, August 1977.
5. Glass, D. E.; Camarda, C. J.; Sena, J. T.; and Merrigan, M. A.: Fabrication and Testing of Heat Pipes for a Heat-Pipe-Cooled Leading Edge, 1997 National Heat Transfer Conference, AIAA 97-3876, Baltimore, MD, August 10-12, 1997.
6. Woloshun, K. A.; Sena, J. T.; Keddy, E. S., and Merrigan, M. A.: Radial Heat Flux Limits on Potassium Heat Pipes: An Experimental and Analytical Investigation, LA-UR-89-3365, 7th Symposium on Space Nuclear Power Systems, Albuquerque, NM, January 7-11, 1990.
7. Woloshun, K. A.; Sena, J. T.; Keddy, E. S., and Merrigan, M. A.: Boiling Limits in Heat Pipes with Annular Gap Wick Structures, LA-UR-89-3943, AIAA/ASME Joint Thermophysics and Heat Transfer Conference, June 18-20, 1990.
8. Keddy, E. A.: Transient Heat Deposition From RF Power Supplies into Heat Pipes, Los Alamos National Laboratory Internal Memorandum MME-13 91-329, June 6, 1991.

REPORT DOCUMENTATION PAGE			Form Approved OMB No. 0704-0188	
Public reporting burden for this collection of information is estimated to average 1 hour per response, including the time for reviewing instructions, searching existing data sources, gathering and maintaining the data needed, and completing and reviewing the collection of information. Send comments regarding this burden estimate or any other aspect of this collection of information, including suggestions for reducing this burden, to Washington Headquarters Services, Directorate for Information Operations and Reports, 1215 Jefferson Davis Highway, Suite 1204, Arlington, VA 22202-4302, and to the Office of Management and Budget, Paperwork Reduction Project (0704-0188), Washington, DC 20503.				
1. AGENCY USE ONLY (Leave blank)		2. REPORT DATE March 1998		3. REPORT TYPE AND DATES COVERED Contractor Report
4. TITLE AND SUBTITLE Start Up of a Nb-1%Zr Potassium Heat Pipe From the Frozen State			5. FUNDING NUMBERS NAS1-19317	
6. AUTHOR(S) David E. Glass, Michael A. Merrigan, and J. Tom Sena			WU 242-33-03-20	
7. PERFORMING ORGANIZATION NAME(S) AND ADDRESS(ES) Analytical Services & Materials, Inc. 107 Research Drive Hampton, VA 23669-1340			8. PERFORMING ORGANIZATION REPORT NUMBER AS&M-S3-98-01	
9. SPONSORING/MONITORING AGENCY NAME(S) AND ADDRESS(ES) National Aeronautics and Space Administration Langley Research Center Hampton, VA 23681-2199			10. SPONSORING/MONITORING AGENCY REPORT NUMBER NASA/CR-1998-207641	
11. SUPPLEMENTARY NOTES Langley Technical Monitor: Steven J. Scotti				
12a. DISTRIBUTION/AVAILABILITY STATEMENT Unclassified-Unlimited Subject Category 34 Distribution: Standard Availability: NASA CASI (301) 621-0390			12b. DISTRIBUTION CODE	
13. ABSTRACT (Maximum 200 words) The start up of a liquid metal heat pipe from the frozen state was evaluated experimentally with a Nb-1%Zr heat pipe with potassium as the working fluid. The heat pipe was fabricated and tested at Los Alamos National Laboratory. RF induction heating was used to heat 13 cm of the 1-m-long heat pipe. The heat pipe and test conditions are well characterized so that the test data may be used for comparison with numerical analyses. An attempt was made during steady state tests to calibrate the heat input so that the heat input would be known during the transient cases. The heat pipe was heated to 675°C with a throughput of 600 W and an input heat flux of 6 W/cm ² . Steady state tests, start up from the frozen state, and transient variations from steady state were performed.				
14. SUBJECT TERMS Heat pipes, liquid metals			15. NUMBER OF PAGES 18	
			16. PRICE CODE A03	
17. SECURITY CLASSIFICATION OF REPORT Unclassified	18. SECURITY CLASSIFICATION OF THIS PAGE Unclassified	19. SECURITY CLASSIFICATION OF ABSTRACT Unclassified	20. LIMITATION OF ABSTRACT	